Applied Catalysis A: General 528 (2016) 113–122

Contents lists available at ScienceDirect

Applied Catalysis A: General

journal homepage: www.elsevier.com/locate/apcata

Enhanced (photo)catalytic activity of Wells-Dawson ($H_6P_2W_{18}O_{62}$) in comparison to Keggin ($H_3PW_{12}O_{40}$) heteropolyacids for 2-propanol dehydration in gas-solid regime

Giuseppe Marcì[a,*], Elisa I. García-López[a], Francesca Rita Pomilla[a,b], Leonarda F. Liotta[c], Leonardo Palmisano[a]

[a] "Schiavello-Grillone" Photocatalysis Group, Dipartimento di Energia, Ingegneria dell'informazione e modelli Matematici (DEIM), Università di Palermo, Viale delle Scienze, 90128 Palermo, Italy
[b] "Dipartimento di Ingegneria per l'Ambiente e il Territorio e Ingegneria Chimica", Università della Calabria via Pietro Bucci 87036 Arcavacata di Rende, Cosenza, Italy
[c] Istituto per Lo Studio dei Materiali Nanostrutturati (ISMN)-CNR, via Ugo La Malfa, 153, 90146 Palermo, Italy

ARTICLE INFO

Article history:
Received 14 May 2016
Received in revised form 9 September 2016
Accepted 3 October 2016
Available online 4 October 2016

Keywords:
Keggin
Wells-Dawson
Heteropolyacid
Polyoxometalate
2-Propanol dehydration
Photocatalysis

ABSTRACT

Catalytic and photocatalytic 2-propanol dehydration to propene at atmospheric pressure and a temperature range of 60–120 °C were carried out in gas-solid regime by using bare and supported Keggin $H_3PW_{12}O_{40}$ (PW_{12}) and Wells-Dawson $H_6P_2W_{18}O_{62}$ (P_2W_{18}) heteropolyacids (HPAs). Binary materials were prepared by impregnation of the HPAs on commercial SiO_2 and TiO_2. The Wells-Dawson was in any case more active than the Keggin heteropolyacid and the differences were enhanced when the supported samples were used. In particular, Wells-Dawson HPA supported on TiO_2 and under irradiation showed the highest activity. The HPA species played the key role both in the catalytic and photo-assisted reactions. The acidity of the cluster accounts for the catalytic role, whereas both the acidity and the redox properties of the HPA species were responsible for the increase of the reaction rate in the photo-assisted catalytic reaction. The estimated apparent activation energy resulted always lower for the photocatalytic process than for the catalytic one.

1. Introduction

Metal oxides can be subdivided into classical solid oxides and nanosized transition metal oxygen clusters, also called polyoxometalates (POMs) [1]. The most explored POM materials are the heteropolyacids (HPAs) which are strong inorganic acids with well-defined molecular structures and it is convenient to classify them as Keggin and Wells-Dawson HPAs, by taking into account the geometry of the heteropolyanion. HPAs are widely used in homo and heterogeneous catalysis [2] and they have been also studied as photocatalysts both in homogeneous [3] and heterogeneous systems [4]. The use of HPAs as catalysts, in both homogeneous and heterogeneous processes, has attracted great interest in organic synthesis because of their stronger Brönsted acidity and redox properties. These materials are also economically and environmentally interesting because inexpensive and non-toxic [5]. Keggin polyanion, $[PW_{12}O_{40}]^{3-}$, is composed of a globe-like cluster whose diameter is ca. 1.0 nm [5,6]. Wells-Dawson heteropolytungstate, $[P_2W_{18}O_{62}]^{6-}$, may be considered derived from two Keggin units by removing a $[W_3O_9]$ block from each of them and by linking these two units by means of oxygen atoms forming a nearly ellipsoidal anion cluster [7]. HPAs show hierarchical structures that result of paramount importance to understand their role as catalysts. The primary structure corresponds to the metal oxide cluster heteropolyanion itself; the secondary structure to the three-dimensional arrangement including counter cations and water molecules. Misono et al. have demonstrated that a solid heteropoly compound can act as catalyst in a gas phase reaction in three different ways, i.e. as (i) surface-type catalyst, (ii) pseudo-liquid bulk-type and (iii) bulk-type catalyst [5,6]. The surface-type catalysis is the ordinary heterogeneous catalysis that takes place bi-dimensionally on the solid surface, in contrast with the bulk-type catalysis. When the diffusion of reactant molecules in the lattice rather than pores of the solid is faster than the reaction, a pseudo-liquid phase is formed in the bulk where the catalytic reaction can proceed. The catalytic behaviour of HPAs is strongly influenced by

* Corresponding author.
E-mail address: giuseppe.marci@unipa.it (G. Marcì).

http://dx.doi.org/10.1016/j.apcata.2016.10.002
0926-860X/

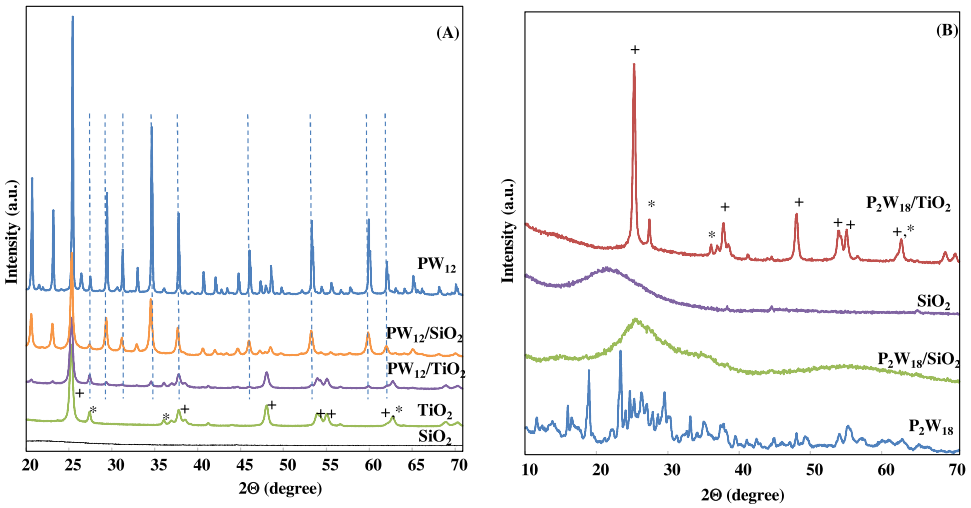

Fig. 1. XRD patterns of the photocatalysts: (A) PW_{12} bare or supported on SiO_2 and TiO_2. and (B) P_2W_{18} bare or supported on SiO_2 and TiO_2. (* Rutile; +Anatase).

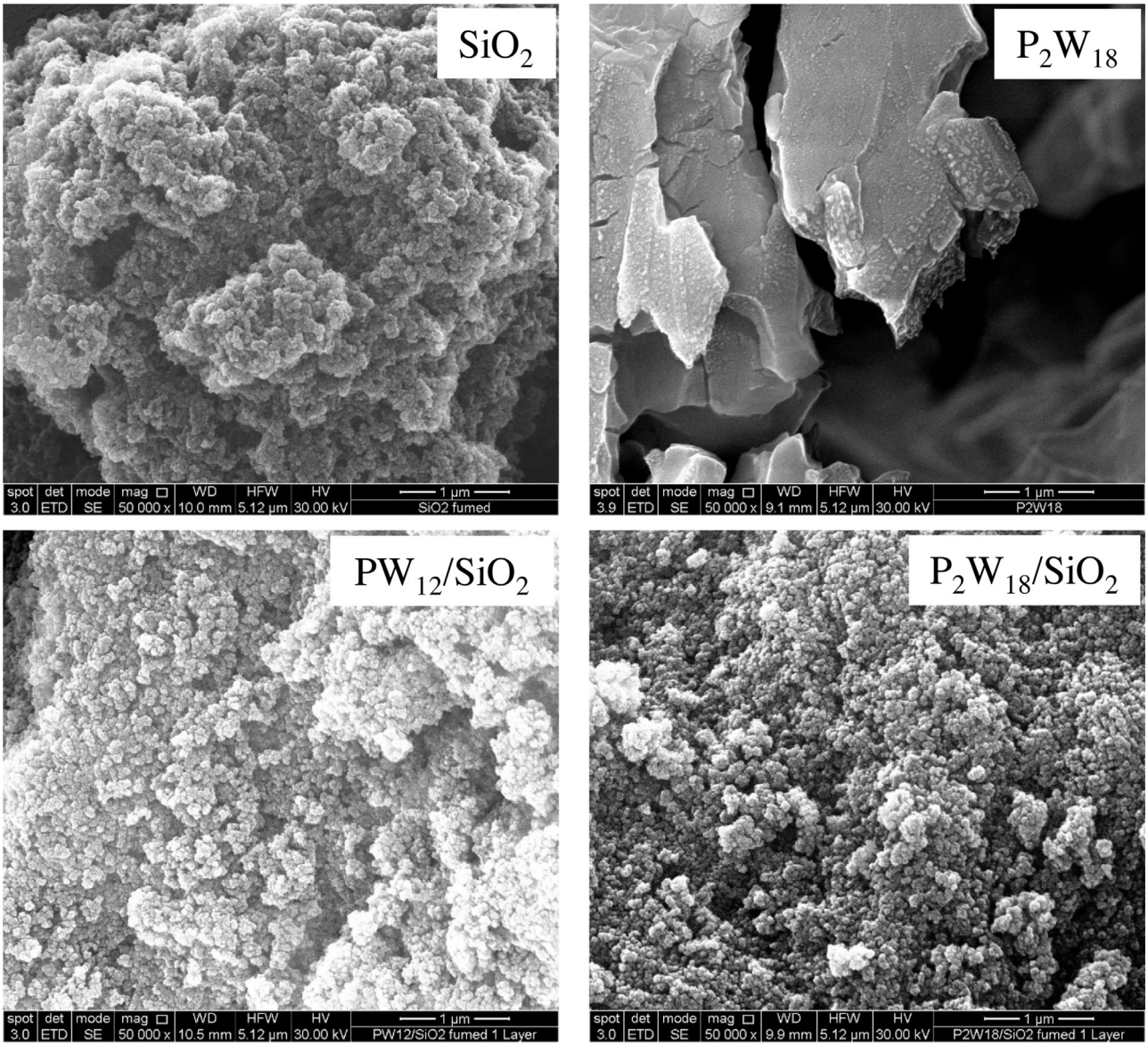

Fig. 2. SEM pictures of bare SiO_2, bare P_2W_{18} and P_2W_{18} and PW_{12} supported on SiO_2.

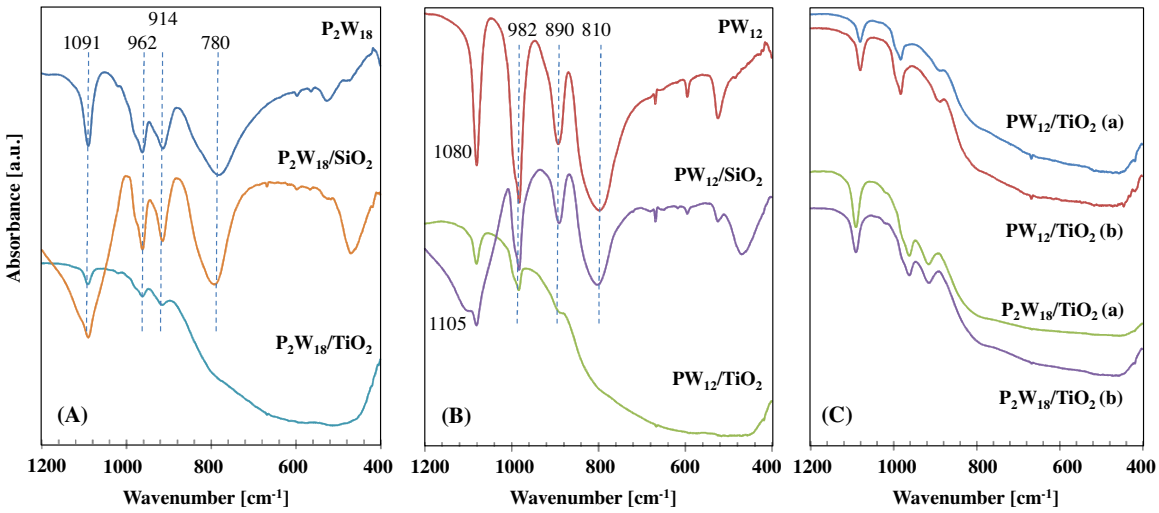

Fig. 3. FTIR spectra of (A) P_2W_{18} bare and supported on SiO_2 and TiO_2; (B) PW_{12} bare and supported on SiO_2 and TiO_2 and (C) PW_{12} and P_2W_{18} supported on TiO_2 after the catalytic (a) and photocatalytic experiments (b), carried out in both cases at 120 °C.

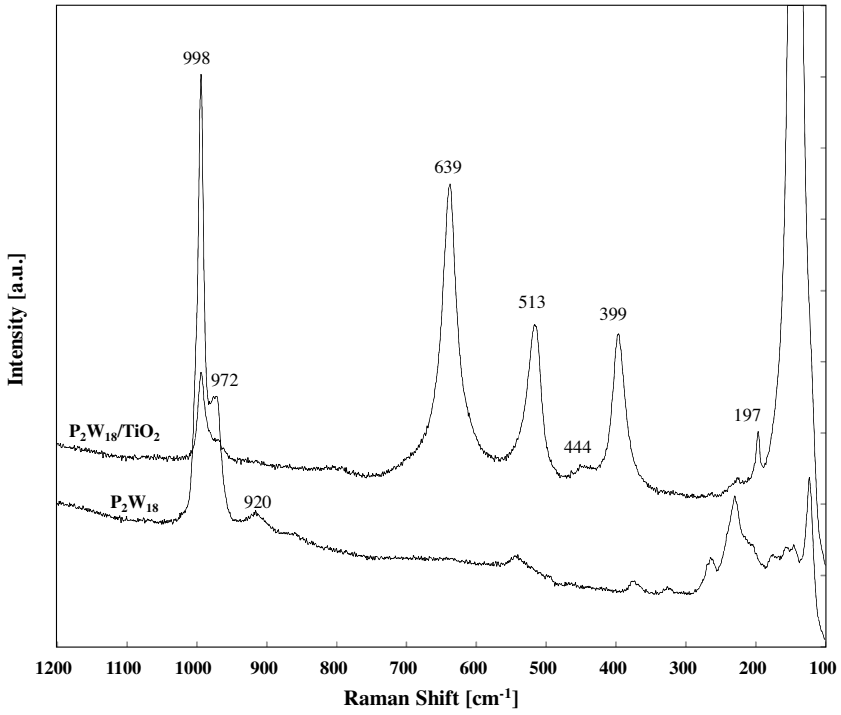

Fig. 4. Raman spectra of the bare P_2W_{18} and P_2W_{18}/TiO_2.

the modifications that may occur in the secondary structure [8] where the Brönsted acidity is located and which would be altered by the number of water molecules involved. The structural modifications that may occur both in the secondary and tertiary structures of the HPAs [2,6–8] influence their hydration state determining the number and strength of the surface acid sites along with the accessibility of the molecules. The acid sites in the secondary structure are $H_5O_2^+$ species.

Baronetti et al. reported the importance of the pseudo-liquid phase formation in Wells-Dawson acid during methyl ter-butyl ether (MTBE) synthesis and methanol dehydration to dimethyl ether in gas phase at 100 °C [9]. The authors observed that the loss of catalytic activity of Wells-Dawson acid with the increase of the pretreatment temperature was due to the loss of water molecules in the secondary structure. The important role of water has been also described for the catalytic behaviour of the Keggin HPA [10]. Among the HPAs, those having Keggin-type structure are currently used in industrial catalytic processes [11], while the Dawson-type HPAs have been used for the selective catalytic oxidative dehydrogenation of isobutene to 2-methyl-propene [12] or for MTBE production [13].

HPAs are used as photocatalysts and their ground electronic state can absorb light producing a charge-transfer excited state (HPA*). This photoexited species can easily become HPA^-, the so-called "heteropolyblue species", by means of electron transfer from another species [3]. Heteropolyblue species (HPA^{n-}) are relatively stable and are readily re-oxidized. The presence of the HPAs supported on different semiconductor oxides has shown a beneficial role in photocatalytic reactions due to the ability of the activated HPA^* species to be reduced by the photoproduced electrons of the

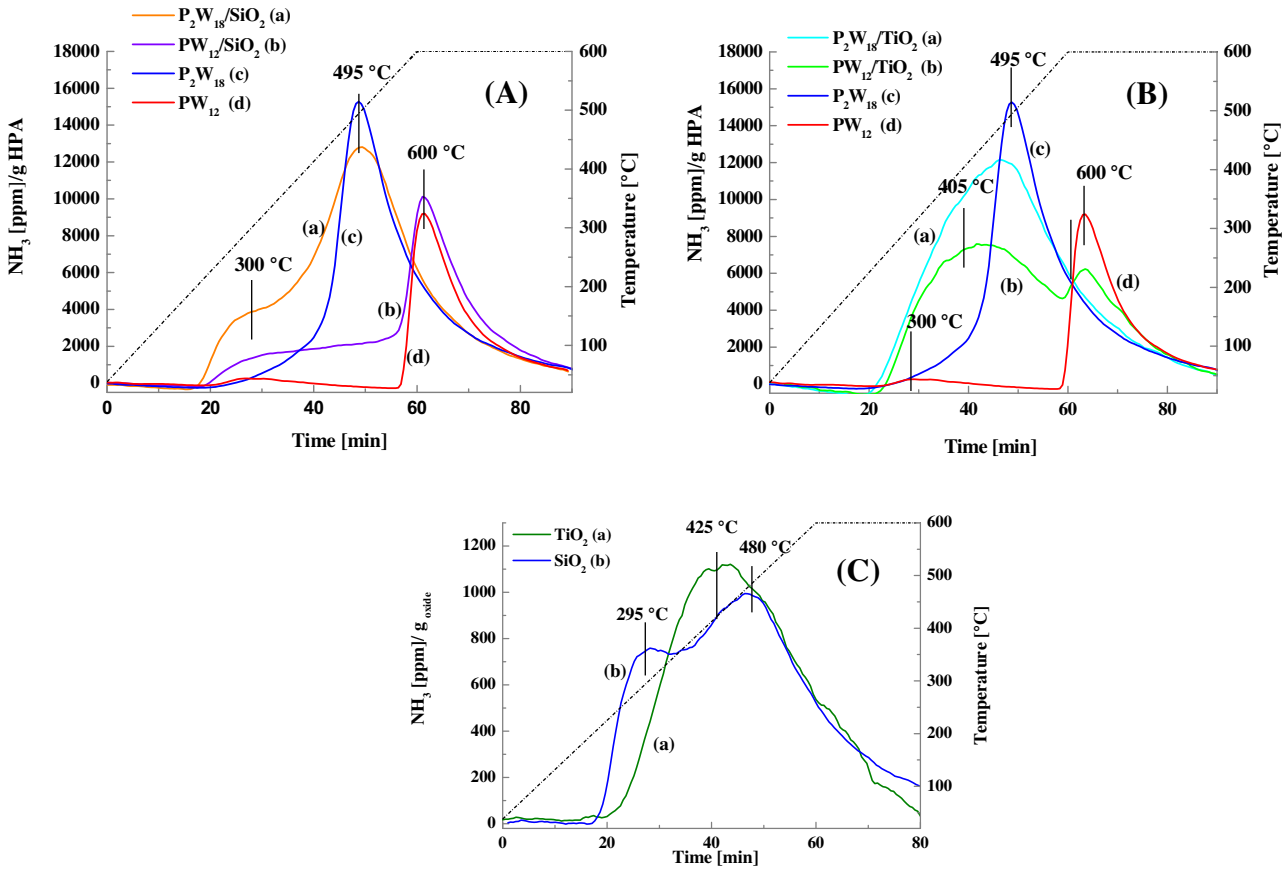

Fig. 5. NH_3-TPD profiles versus time and temperature for SiO_2 supported HPAs (A), for TiO_2 supported HPAs (B), and for bare SiO_2 and TiO_2 (C). Bare P_2W_{18} and PW_{12}, were inserted for comparison in (A) and (B).

conduction band of the UV-activated semiconductor [14–18]. The redox potentials of Wells-Dawson and of Keggin HPA both in the ground and even better in the excited state are suitable to allow electron transfer from the conduction band of TiO_2.

In this paper the (photo)catalytic 2-propanol dehydration to propene in gas-solid regime has been carried out by using two types of HPAs, i.e. $H_3PW_{12}O_{40}$ or $H_6P_2W_{18}O_{62}$ both bare and deposited on SiO_2 or TiO_2. Some bulk and surface properties of the solids have been studied and both their catalytic and photocatalytic activity investigated. The research aimed to understand the role of the HPA on the catalytic process and how the modified physico-chemical properties of the supported HPAs give rise to different (photo)catalytic activities with respect to the bare ones.

2. Experimental

2.1. Preparation of the binary heteropolyacid/support samples

Two sets of catalysts have been prepared by using two types of heteropolyacid clusters (HPAs). The Keggin, $H_3PW_{12}O_{40}$, (Aldrich 99.7%) was labelled as PW_{12}. The Wells-Dawson heteropolyacid, $H_6P_2W_{18}O_{62}$, labelled as P_2W_{18}, was synthetized in the laboratory. It was obtained through the synthesis of $K_6P_2W_{18}O_{62}$ salt: H_3PO_4 acid (2 ml) was added to a solution of $NaWO_4$ (0.01 mol) in water (30 ml) and the solution was refluxed for 8 h. The salt was precipitated by adding KCl (1 g) and purified by recrystallization (t = 5 °C). The product was filtered, washed and then vacuum-dried for 8 h [9,19,20]. The salt was transformed in phosphotungstic Wells-Dawson acid, $H_6P_2W_{18}O_{62}$, according to the "etherate method" [9].

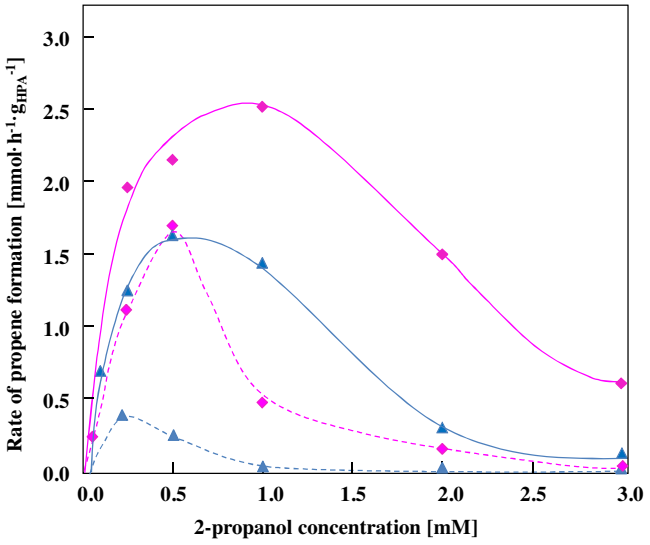

Fig. 6. Reaction rate of propene formation per gram of HPA versus 2-propanol concentration for runs carried out by using bare PW_{12} (▲) and bare P_2W_{18} (◆) as catalysts (dotted line) or as photocatalysts (full line). Flow rate of the feeding gas equal to 100 mL min^{-1}, temperature 80 °C and 0.5 g of catalyst.

This process implies the addition of ether and concentrated HCl (37%) to an aqueous solution of the α/β mixture of the $K_6P_2W_{18}O_{62}$ salt. $H_6P_2W_{18}O_{62}$ formed a compound with ether, which can be separated by extraction. The ether solution, containing the HPA,

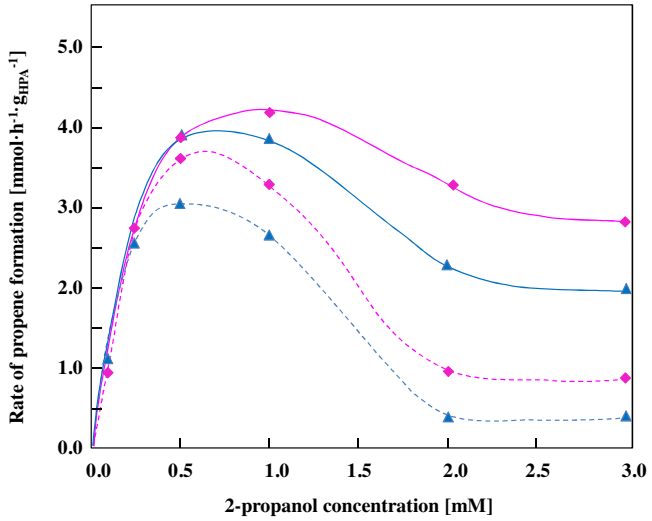

Fig. 7. Reaction rate of propene formation per gram of HPA versus 2-propanol concentration for runs carried out by using PW_{12}/SiO_2 (▲) and P_2W_{18}/SiO_2 (◆) as catalysts (dotted line) or as photocatalysts (full line). Flow rate of the feeding gas equal to 100 mL min^{-1}, temperature 80 °C and 0.5 g of catalyst.

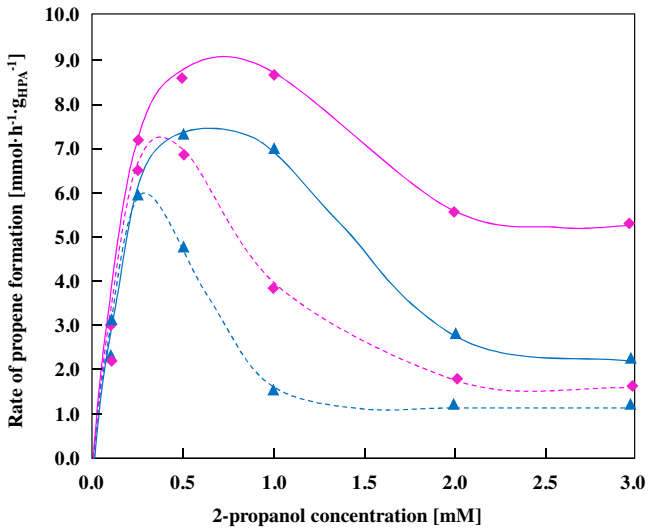

Fig. 8. Reaction rate of propene formation per gram of HPA versus 2-propanol concentration for runs carried out by using PW_{12}/TiO_2 (▲) and P_2W_{18}/TiO_2 (◆) as catalysts (dotted line) or as photocatalysts (full line). Flow rate of the feeding gas equal to 100 mL min^{-1}, temperature 80 °C and 0.5 g of catalyst.

was placed in a vacuum-desiccator until crystallization of the HPA as a polycrystalline solid.

Both PW_{12} and P_2W_{18} have been supported by impregnation on commercial SiO_2 (fumed, Aldrich) or TiO_2 (Evonik P25). SiO_2 or TiO_2 were added to an aqueous solution of PW_{12} or P_2W_{18}. The resulting suspension was stirred, dried and annealed at 50 °C overnight. The aqueous HPA suspensions contained a sufficient amount of PW_{12} or P_2W_{18} to theoretically form ca. one monolayer onto the oxide surface, as detailed in the "Results and discussion" section. The resulting powders were labelled as PW_{12}/SiO_2 and P_2W_{18}/SiO_2 or PW_{12}/TiO_2 and P_2W_{18}/TiO_2.

2.2. Characterization of the binary heteropolyacid/support samples

Bulk and surface characterizations were carried out in order to define some physicochemical properties of the powders. The crystalline structure of the samples was determined at room temperature by powder X-ray diffraction analysis (PXRD) carried out by using a Panalytical Empyrean, equipped with CuKa radiation and PixCel1D (tm) detector. Scanning electron microscopy (SEM) was performed by using a FEI Quanta 200 ESEM microscope, operating at 20 kV on specimens upon which a thin layer of gold had been evaporated. An electron microprobe used in an energy dispersive mode (EDX) was employed to obtain information on the actual metal content present in the samples in order to evaluate the overall dispersion of the HPA on the support. Specific surface area and porosity were determined in accordance with the BET method from the nitrogen adsorption-desorption isotherm using a Micromeritics ASAP 2020. The structure of the HPA and the preservation of the cluster structure after the deposition and the (photo)reactivity experiments were studied by vibrational spectroscopy. FTIR spectra of the samples in KBr (Aldrich) pellets were obtained by using a FTIR-8400 Shimadzu spectrometer with 4 cm^{-1} resolution and 256 scans. Raman measurements were performed on pure powdered samples. The spectra were recorded by a Reinshaw in-via Raman equipped with an integrated microscope and with a charge-coupled device (CCD) camera. A He/Ne laser operating at 632.8 nm was used as the exciting source.

The acidity of the (photo)catalysts was determined by temperature-programmed desorption of ammonia (NH_3-TPD) experiments by using a Micromeritics Autochem 2950 apparatus equipped with a thermal conductivity detector (TCD), a quadrupole mass (QM) spectrometer (Ther-mostar, Balzers) and an ultraviolet gas analyzer (ABB, Limas 11). The sample amount of 0.3 g was pretreated in He flow at 100 °C for 30 min. Then, after cooling down to room temperature, ammonia adsorption was performed by admitting a flow of 5% NH_3/He stream (30 ml min^{-1}) for 1 h. In order to remove all the physically adsorbed ammonia, the sample was purged by flowing 100 ml min^{-1} He at 100 °C for 1 h. Then, after cooling down to room temperature, ammonia desorption started by flowing He (30 ml min^{-1}) and heating up to 600 °C (rate of 10 °C min^{-1}), holding time at 600 °C for 30 min. Ammonia concentration profiles were recorded with the ultraviolet gas analyzer. TCD and QM data were used to qualitatively confirm the trends.

2.3. Catalytic and catalytic photo-assisted experiments

The reactivity set-up consisted of a cylindrical continuous Pyrex photoreactor horizontally positioned (diameter: 10 mm, length: 100 mm). The reactivity experiments were carried out with 0.5 g of solid powder placed as a thin layer inside the (photo)catalytic reactor. A porous glass septum allowed to homogeneously distribute the gaseous inlet mixture. It consisted of a nitrogen flow containing 2-propanol with a concentration ranging between 0.1 and 3.0 mM. A mass flow controller allowed the N_2 feeding, whereas 2-propanol was added in the N_2 stream by means of a home assembled infusion pump. The flow rate of the gaseous stream for both the catalytic and photocatalytic runs was 100 ml min^{-1}. All the runs have been carried out at atmospheric pressure. The reactor and the pipes of the whole set-up, including the reactor, were heated by an electric resistance. K-type thermocouples allowed to monitor the temperature in the system. The temperature inside the (photo)-reactor was modified in the range 60–120 °C both for catalytic and catalytic photo-assisted experiments. For the photocatalytic runs the reactor was illuminated from the top by two UV LED IRIS 40 lamps with an irradiation peak centred at 365 nm. The irradiance reaching the reactor, measured in the range 300–400 nm by a UVX Digital radiometer, resulted 0.50 W. The temperature of the photoreactor did not increase due to the irradiation by LEDs. A pretreatment of the catalysts was carried out under N_2 at 60 °C for 0.5 h. The runs lasted ca. 8 or 24 h and samples of the reacting fluid were analyzed by a GC-2010 Shimadzu gas chromatograph equipped with a Phe-

nomenex Zebron Wax-plus column (30 m × 0.32 μm × 0.53 μm) and a flame ionization detector, using He as the carrier gas.

Preliminary runs indicated that the presence of the heteropolyacid is essential for the conversion of 2-propanol in the (photo)catalytic reactions. No activity was observed in the presence of bare SiO_2 or TiO_2. The occurrence of the reaction needed $t \geq 60\,^{\circ}C$ both under dark and irradiation conditions.

3. Results and discussion

3.1. Bulk and textural photocatalysts characterization

Diffractograms of the Keggin based materials along with the bare oxides are reported in Fig. 1(A). Bare PW_{12} presents a crystalline structure characterized by several diffraction peaks. Anatase and rutile polymorphs can be identified in the commercial TiO_2 P25 diffractogram, whereas SiO_2 resulted amorphous. The main peaks attributable to the Keggin HPA along with those related to anatase and rutile are present in the PW_{12}/TiO_2 composite. The diffraction of the PW_{12}/SiO_2 material shows the main peaks attributed to the HPA. Diffractogramms related to the Wells-Dawson HPA along with its composites are reported in Fig. 1(B). The shape of Dawson-type heteropolyanion is not spherical as the Keggin-type one and its secondary structure is less ordered resulting in a complicated diffactogram, as reported before [9,21]. This can be deduced from XRD spectra, which presented less symmetry. This phenomenon has been previously observed also for the Keggin structure when the secondary structure was altered after an annealing process [22]. The HPAs peaks cannot be observed neither in P_2W_{18}/TiO_2 nor in P_2W_{18}/SiO_2, due to their good dispersion on the surface of the support, as confirmed by SEM.

SEM microphotographs of PW_{12} and P_2W_{18} supported materials show the characteristic morphology of the support used. Fig. 2 reports pictures of bare SiO_2, bare P_2W_{18} and both PW_{12} and P_2W_{18} supported on SiO_2. It can be noticed how the morphology of the supported materials is very similar to that of the support. On the contrary, PW_{12} (picture not reported for the sake of brevity) and P_2W_{18} lost their morphology when impregnated on the support because they were well dispersed on SiO_2. The same behaviour was observed for the PW_{12} and P_2W_{18} supported on TiO_2 (pictures not reported).

As far as the EDX measurements are concerned, they allowed to obtain information on the actual HPA content only for the TiO_2 based samples because the overlapping of Si and W signal in SiO_2 based catalyst did not allow to properly analyse the percentage of Si and W. Anyhow, the measured HPA/TiO_2 ratios for both the impregnated samples were very close to the nominal ones showing small oscillations between various determinations in different areas of the samples, indicating a good dispersion of HPA. Table 1 reports all of the samples used in the current research along with some physico-chemical parameters, the mass percentage of the HPA present in each binary material and the theoretical HPA coverage.

The specific surface areas (SSA) of the oxides impregnated with the HPAs decreased with respect to the bare oxides, in agreement with previous studies [23] and this was more evident for the Wells-Dawson cluster, as shown in Table 1. This decrease was more significant in the case of HPAs supported on SiO_2. The block of some pores of the supports, due to the presence of the HPA clusters, could account for this result. The observed increase of the diameter of the pores could be explained by considering the formation of new pores when HPA was supported. Consequently, the presence of HPA blocks the smaller pores of the support but induces the formation of new larger pores.

The amounts of HPAs needed to form the theoretical coverage of the support has been calculated by taking into account the size of the HPAs primary structures and the specific surface areas of the supports (these values are reported in Table 1). The diameter of the Keggin is equal to ca. 10 Å and by considering a roundish shape, each cluster results ca. 78.5 $Å^2$ [5]. According to Sambeth et al. [24] the parameters of the primary Wells-Dawson HPA structure can be assumed as a rectangular prism sized (21.5 × 15.5 × 12.1) Å; consequently the area occupied by each cluster resulted ca. 94 and 167 $Å^2$ by considering the upright and reclined species, respectively.

FTIR experiments were useful to evaluate the presence of the Wells-Dawson structure which was a home prepared HPA, but also to confirm the retention of both Keggin and Wells-Dawson cluster structures after the dispersion of the HPA onto the oxide surface. The FTIR spectrum of the P_2W_{18}, shown in Fig. 3(A), presents the following strong vibration bands: 1091 cm^{-1} attributed to the ν_{as} frequency of the PO_4 tetrahedron, 962 cm^{-1} to the ν_{as} of the terminal W—O bonds and two bands at 914 and 780 cm^{-1}, assigned to the ν_{as} vibration of the W—O—W bridges, in agreement to the Wells-Dawson HPA spectrum reported in the literature [25]. The dispersion of P_2W_{18} on SiO_2 and TiO_2 did not shift the vibrational modes of the Wells-Dawson HPA, indicating the preservation of the cluster structure.

Both Raman and FTIR spectra confirm the Wells-Dawson structure of the home prepared P_2W_{18}. The FTIR spectra confirmed the retention of both Keggin and Wells-Dawson structures after the dispersion of the HPA onto the support.

The spectrum of the bare PW_{12} showed in Fig. 3(B), presents four characteristic bands [26,27] at 1080, 982, 890, 810 cm^{-1} corresponding to ν_{as}(P-O_a), ν_{as}(W-O_d), ν_{as}(W-O_b-W) and ν_{as}(W-O_c-W), respectively. For spectra of the supported PW_{12} samples, reported in Fig. 3(B), the Keggin anion skeletal vibrations were observed at the same frequencies than for the bare PW_{12}, indicating the retention of the Keggin structure in the binary material. In the PW_{12}/SiO_2 spectra, the band at 1105 is attributed to SiO_2. Concerning the PW_{12}/TiO_2 sample, the Ti-O bonds in the TiO_2 P25 Evonik gave rise to an absorption spectrum in the range 900 to 700 cm^{-1}, dominating part of the spectrum.

Remarkably, all of the supported materials showed no important differences in the FTIR spectrum before and after the catalytic or the photocatalytic experiments, as reported in Fig. 3(C). The spectra of the catalytically or photocatalytically used PW_{12} and P_2W_{18} supported on TiO_2, showed neither shifts nor differences in relative intensity of the bands or additional bands with respect to the freshly prepared samples. With this respect, it has been reported that the modification of the secondary structure of the HPAs, for instance by a partial loss of water, increases the disorder in the secondary structure, hence inducing the bands at 911 and 778 cm^{-1} to become broader and with lower intensities [25]. The primary structure remains stable, although the distance between the primary units can change. This behaviour was not observed, as both HPAs maintained their secondary structure after catalytic and photocatalytic reactions even after 120 °C. This finding can be explained by taking into account that the dehydration reaction produced water molecules that maintained an extent of hydration sufficient for the Brönsted sites to be still active.

As far as the Raman vibrational spectra are concerned, the Wells-Dawson heteropolyanion exhibits multiple W_dO vibrations between 950 and 1005 cm^{-1}, reflecting a distribution of distortions among the WO_6 units in the framework. Those species possess a strong Raman signal at 998 cm^{-1} corresponding to the ν_s of the terminal W—O bonds, along with other signals of lower intensity at 972, 920 and 853 cm^{-1}, attributed to ν_{as} of the terminal W-O bonds, ν_{as} of bridging W-O-W and ν_{as} of O-W-O bonds of the extended polytungstate framework surrounding the central PO_4 group [27]. The Raman spectrum of the home prepared Wells-

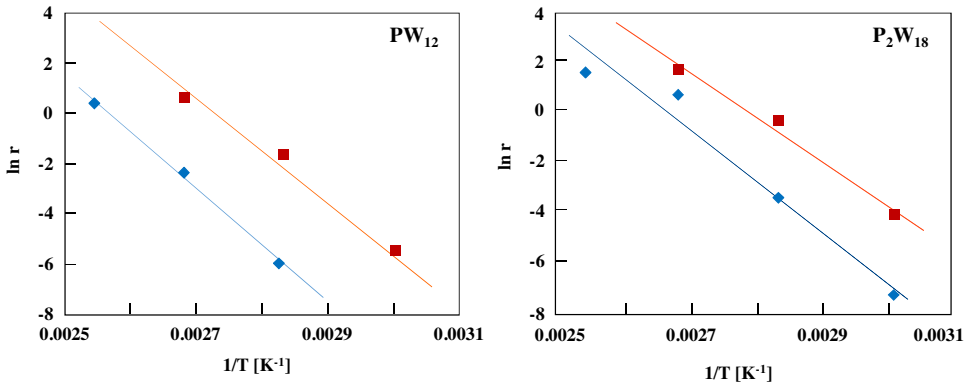

Fig. 9. Plots of "*ln r*" versus "*1/T*" used to calculate "E_a" and "*ln A*". Experiments carried out by using the bare HPAs as catalysts (♦) or photocatalysts (■). The units of "*r*" are mmol h^{-1} g^{-1}_{HPA}.

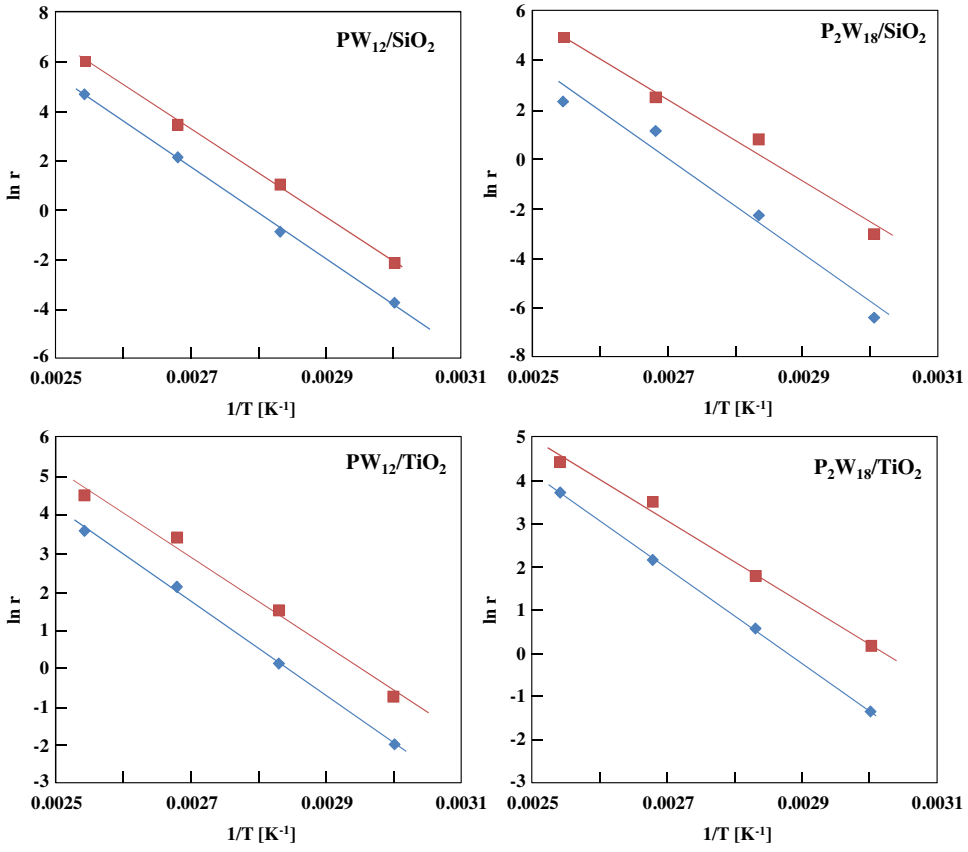

Fig. 10. Plots of "*ln r*" versus "*1/T*" used to calculate "E_a" and "*ln A*". Experiments carried out by using the SiO_2 and TiO_2 supported HPAs as catalysts (♦) or photocatalysts (■). The units of "*r*" are mmol h^{-1} g^{-1}_{HPA}.

Table 1
BET specific surface area (SSA), pore size, mass percentage of HPA on the binary material, theoretical HPA coverage on the support.

Sample	SSA [m^2 g^{-1}]	Pore size [nm]	Mass percentage of HPA [%]	Theoretical HPA coverage
SiO_2	319	9.5	–	–
TiO_2	56	22.5	–	–
PW_{12}	15	–	–	–
P_2W_{18}	5	–	–	–
PW_{12}/SiO_2	53	25.2	70	1.1
PW_{12}/TiO_2	50	28.8	26	0.9
P_2W_{18}/SiO_2	38	28.5	70	0.8–1.4[a]
P_2W_{18}/TiO_2	46	24.9	26	0.7–1.3[a]

[a] Values calculated by considering two different positions of the species on the surface of the support: upright or reclined.

Table 2
Apparent activation Energy (E_a) and logarithm of the pre-exponential factor (ln A) for catalytic and photocatalytic 2-propanol dehydration.

	E_a [kJ/mol]		ln A	
Catalyst	Catalytic	Photocatalytic	Catalytic	Photocatalytic
PW_{12}	186	157	56	50
PW_{12}/SiO_2	151	144	51	50
PW_{12}/TiO_2	101	96	35	34
P_2W_{18}	175	152	56	51
P_2W_{18}/SiO_2	161	139	52	47
P_2W_{18}/TiO_2	92	86	32	31

Dawson heteropolyacid P_2W_{18} is shown in Fig. 4. The selected sample P_2W_{18}/TiO_2, shown for the sake of comparison, confirmed the upshifted position of the vibrational modes, in accord with the FTIR conclusions regarding the preservation of the cluster after the dispersion onto the oxides surface. Moreover, Fig. 4 shows characteristic Raman vibrational modes of the TiO_2 anatase centered at 144, 197, 399, 513, and 639 cm^{-1}, attributable to the E_g, E_g, B_{1g}, A_{1g} and B_{2g} [28]. A peak attributed to the rutile phase is also present and located at 444 cm^{-1}. Intense peaks at 142 and 144 cm^{-1}, assigned to rutile and anatase, respectively, are out of the range of the spectra reported.

The acid properties of HPAs supported samples were evaluated by NH_3-TPD experiments carried out from room temperature up to 600 °C. Such high temperature was chosen in order to detect also the contribution of strong acid sites that are known to desorb NH_3 above 550 °C. According with the literature we were confident that in the selected range of temperature both Keggin and Dawson acids still keep their heteropolyoxoanion structure [9,10].

The technique provides information on the total acidity of the catalysts without distinguishing between Brönsted acid sites (typical of HPAs and SiO_2) and Lewis acid sites, characteristic of defective TiO_2 support. The amount of NH_3 desorbed (ppm/g HPAs) gives a quantitative evaluation of the number of active sites, while the temperature of desorption is an indication of the strength of the acid sites. In Fig. 5(A)–(C) the NH_3-TPD profiles are displayed for bare HPAs, for SiO_2 and TiO_2 supported HPAs and for bare supports, respectively. No NH_3 desorption occurs at temperature below 200 °C, suggesting the absence of weak acid sites [23,29]. For bare and SiO_2 supported P_2W_{18} the main desorption occurs with a broad and intense peak centred at 495 °C corresponding to 15,260 and to 12,780 ppm of NH_3 desorbed per gram of HPA, respectively. According with our previous results [29] NH_3 desorption in the range 200–550 °C has been attributed to medium strength acid sites. A pronounced shoulder at around 300 °C was also detected for P_2W_{18}/SiO_2. By comparison with the profile of bare P_2W_{18} and that of bare SiO_2 support it can be concluded that such low temperature feature is due to the contribution of SiO_2 medium acid sites. Moreover, a careful analysis of the TPD curves suggests for both samples, P_2W_{18} and P_2W_{18}/SiO_2, the presence of some strong acid sites. Unlike P_2W_{18} samples, in the case of bare and SiO_2 supported PW_{12} the main desorption peak of ammonia (around 10,000 ppm/g HPA) was detected at 600 °C confirming that the acid sites in Keggin-type heteropolyacids are stronger than that of Dawson-type HPAs [30]. By looking at the NH_3-TPD curves of TiO_2 supported HPAs, a broad peak centered at around 450 °C was observed for both samples. Along with such features, attributed to the Lewis acid sites typical of TiO_2 (see Fig. 5(C)) [31], the peaks corresponding to the Brönsted acid sites of the HPAs were clearly detected at 495 (12,200 ppm of NH_3/g HPA) for P_2W_{18}/TiO_2 and at 600 °C (~6000 ppm NH_3/g HPA) for PW_{12}/TiO_2.

3.2. Catalytic and photocatalytic reactivity

The presence of the heteropolyacid is essential for the dehydration of 2-propanol both in catalytic and photocatalytic reactions; in fact, no activity was observed in the presence of both bare TiO_2 and SiO_2 samples. Moreover, the occurrence of the reaction needed $t \geq 60$ °C both under irradiation and dark conditions. Preliminary runs indicated that it was necessary to feed the (photo)reactor with a flow rate of 100 mL min^{-1} in order to work under kinetic regime conditions.

Catalytic and photocatalytic experiments were carried out at different initial 2-propanol concentrations and by using both the bare and supported HPAs. Propene and di-isopropyl ether were the main reaction products observed both in the absence and in the presence of UV light, but the extent of ether formation was generally much lower with respect to that of propene (ca. one order of magnitude less, under irradiation). This finding indicates that the selectivity of the 2-propanol dehydration reaction versus propene formation ranged between 85 and 93% in the absence or in the presence of light, respectively. These values were approximately the same for all of the catalysts used. The rate of propene formation per gram of HPA versus 2-propanol concentration in the feeding stream is reported in Fig. 6 for runs carried out by using bare PW_{12} or P_2W_{18} as the (photo)catalysts.

In all of the experiments, the rate of propene formation firstly increased and then decreased by increasing 2-propanol concentration. Consequently, a maximum substrate concentration exists above which a dramatic decrease of reactivity occurs. HPAs present the uncommon ability to absorb polar substrates in their bulk giving rise to catalytic reactions in the "pseudo-liquid" phase [5,6]. Therefore the solubility of 2-propanol in the water molecules of the secondary structure of the HPA should be invoked to explain their reactivity. This phenomenon has been observed for the catalytic formation of tertiary ethers in gas phase by addition of polar alcohols (methanol or ethanol) to isobutene for experiments carried out with $H_4SiW_{12}O_{40}$ and $H_6P_2W_{18}O_{62}$ [32] or in the presence of PW_{12} and P_2W_{18} [8,13]. The same phenomenon was observed by using bare and supported $H_3PW_{12}O_{40}$ in the catalytic and photocatalytic 2-propanol dehydration [33]. In Fig. 6 it can be observed that the reaction rate decrease started at lower 2-propanol concentration for the catalytic experiments than for the photocatalytic ones. Moreover, Wells-Dawson HPA material was more active than the Keggin one.

According to the literature, the catalytic dehydration of 2-propanol occurs by means of an acid-base mechanism (elimination E1) involving the dioxonium ions placed between the HPA anions [33,34]. Consequently, the amounts of acid sites present in the catalysts should account for their activity. The NH_3-TPD experiments in accord with the reactivity results, indicate that P_2W_{18} shows higher amount of acid sites with respect to PW_{12}. Here it is important to underline that, although it is reported the higher catalytic activity of the Wells-Dawson HPA material with respect to the Keggin one, this finding is considered surprising because the adsorption heat of NH_3 (evaluated by microcalorimetry) indicates the presence of stronger acid sites in Keggin HPA [6,30,32].

The NH_3-TPD study reported in this work confirmed that PW_{12} presents stronger acid sites with respect to P_2W_{18}. However, the average amount of acid sites in P_2W_{18} (0.33 $mmol_{NH3}$ $g^{-1}{}_{HPA}$) is significantly higher than that in PW_{12} (0.13 $mmol_{NH3}$ $g^{-1}{}_{HPA}$). Consequently, the activity of the samples should be related not only to the strength of the acid sites but also to their amount.

By irradiating the system, the reaction rate of propene formation increased for both HPAs and the 2-propanol concentration corresponding to the maximum reactivity shifted to a higher substrate concentration (from 0.25 to 0.5 mM for PW_{12}, and from 0.5 to 1 mM for P_2W_{18}), as showed in Fig. 6. The increase of the reactivity under

UV irradiation will be explained later along with the behaviour of the supported samples.

The catalytic and photocatalytic propene formation rates per gram of HPA in the presence of SiO_2- and TiO_2-supported HPAs versus the concentration of 2-propanol in the feeding stream are reported in Figs. 7 and 8, respectively. The overall catalytic and photocatalytic behaviours of the supported PW_{12} and P_2W_{18} were similar to those observed for the bare HPAs, indicating that the dehydration reaction occurred in the pseudo-liquid phase also for the supported HPAs. Consequently, as reported in Figs. 7 and 8, the rate of propene formation firstly increased (reaching a maximum) and then decreased by increasing 2-propanol concentration when the supported samples were used as the (photo)catalysts. The supported Wells-Dawson HPAs were more active than the analogous Keggin HPAs for the catalytic process, although the activities of the supported samples were very similar at the lowest 2-propanol concentration. The different catalytic activity of PW_{12} and P_2W_{18} supported samples could be related, as for the bare HPAs, to the higher amounts of acid sites present on the P_2W_{18} supported catalysts. Propene formation rate increased under UV irradiation for all of the solids and the supported P_2W_{18} samples were always the most active ones. Notably 2-propanol conversion always decreased by increasing 2-propanol concentration in the feeding gas, being averagely ca. 70% and 8% for the lowest and the highest concentrations, respectively, for both types of supported catalysts.

A perusal of Figs. 6–8 indicates that the reaction rates of propene formation in the presence of HPAs/SiO_2 or HPAs/TiO_2 samples were higher than in the presence of bare HPAs, both for catalytic and photocatalytic experiments.

The increase of the activity of the supported materials with respect to the bare ones can be explained by considering the higher SSA values of these samples accounting for a larger surface of contact between the cluster and 2-propanol.

Notably, the reaction rate decrease vs. 2-propanol concentration in the feeding stream was more dramatic for the catalytic than for the photocatalytic experiments. As shown in Figs. 6–8, it is impossible to find a unique concentration of 2-propanol for which the reactivity was maximum, however the 1 mM concentration resulted a good compromise in order to compare the reactivity of the various samples. By studying the activity results reported in Figs. 7 and 8 for runs carried out at 2-propanol concentration equal to 1 mM, it can be concluded that: (i) the activity under dark condition in the presence of PW_{12}/SiO_2 was higher than that observed with the PW_{12}/TiO_2 sample; (ii) the activity under dark condition by using P_2W_{18}/SiO_2 was very similar than that obtained in the presence of P_2W_{18}/TiO_2 samples; (iii) the activity under irradiation of the HPAs supported on TiO_2 was always higher than that of the corresponding HPAs/SiO_2 samples. The NH_3-TPD study indicates that, among the supported samples, PW_{12}/SiO_2 and PW_{12}/TiO_2 were the less acidic ones (the total amount of ammonia desorbed was 0.24 and 0.36 $mmol_{NH3}\ g^{-1}{}_{HPA}$, respectively), whereas P_2W_{18}/SiO_2 and P_2W_{18}/TiO_2 showed very similar acidity (0.44 and 0.46 $mmol_{NH3}\ g^{-1}{}_{HPA}$, respectively) that was higher than that observed for the corresponding supported PW_{12} samples (see also Fig. 5). These findings are in good agreement with the reactivity showed under dark conditions, i.e. the catalytic experiments, indicating that the most important factor controlling the reactivity is the acidity of the catalyst. The UV irradiation clearly gave rise to an increase of the performance of both HPAs, which was significantly higher for the samples supported on TiO_2. The beneficial role of UV irradiation in the dehydration reaction of 2-propanol to propene carried out in the presence of bare and hydrothermally prepared supported PW_{12} was previously reported [33]. Briefly, during the catalytic photo-assisted reactions, in addition to the previous mentioned acid-base mechanism, a further key role is played by both HPAs (PW_{12} and P_2W_{18}). Indeed, HPA after photosensitization can trap an electron from 2-propanol giving rise to the heteropolyblue species (see Introduction Section). Notably, all materials containing HPAs become strongly blue coloured under irradiation only in the presence of 2-propanol. The further hypothesized evolution of 2-propanol radical species to propene is reported in [33].

The fact that TiO_2 showed to be the best support in the photocatalytic reaction suggests the occurrence of a synergistic effect in which the 2-propanol radical species formed as above reported are reduced to propene by trapping photo-generated electrons in the conduction band of TiO_2 and contemporaneously the heteropolyblue species are re-oxidized to HPAs [33]. Moreover, it can not be excluded that the photosensitized HPA possesses an oxidation potential sufficient to abstract a photogenerated electron from the conduction band of TiO_2. Such electron transfer could (i) produce a higher number of HPA^- species and (ii) inhibit the fast electron-hole recombination on TiO_2 [16,18]. Nevertheless, these two effects should result very useful when TiO_2 is used as the photocatalyst (for oxidation reaction) but not in this work in which the active phases were the HPA species. The increase of the reactivity observed under irradiation was sometimes very high, and similar performances were achieved only when the temperature for catalytic reactions was ca. 15–20 °C higher with respect to the photocatalytic ones.

Interestingly, some runs carried out for long time (ca. 24 h) showed that the reactivity and the selectivity of the catalysts did not change indicating a good stability of these samples.

The reactivity study of the supported samples, as above reported, was carried out by using catalysts prepared with the same theoretical HPA coverage, i.e ca. 1 monolayer, both on TiO_2 and SiO_2, because the aim of this work was to compare the reactivity of two heteropolyacids both bare and supported with the same coverage in two different oxides. Anyway, for the sake of completeness two additional samples were prepared in which HPAs were supported on SiO_2 with a weight percentage of 26% (the same used for the HPAs/TiO_2 samples) and they were tested to compare also the reactivity of supported samples with the same HPA percentage. For these two samples, whose the theoretical coverage of PW_{12} or P_2W_{18} on SiO_2 was ca. 0.2 monolayer, the (photo)catalytic tests were carried out only with 1 mM 2-propanol in the feeding gas. The results, not reported for the sake of brevity, indicated that the (photo)reactivity figures were lower than those of the corresponding HPAs/SiO_2 samples with the highest percentage of HPAs when the whole catalyst mass was considered, but they showed to be higher per gram of heteropolyacid. Moreover, the (photo)reactivity was very similar to that showed by the HPAs/TiO_2 samples. This finding indicates that a more detailed study on the HPA coverage is needed in the future to establish what is the most performing catalyst.

3.3. Study on the apparent activation energy of the catalytic and catalytic photo-assisted reactions

The apparent activation energy of 2-propanol dehydration reaction to propene has been estimated by applying the Arrhenius equation by considering a zero order rate reaction. The experiments at increasing temperature were carried out at concentration of 2-propanol equal to 3 mM because, as showed in Figs. 7 and 8, at this concentration the reaction rate of propene formation was in a plateau by using all of the (photo)catalysts and 2-propanol conversion was less than 10%. This finding indicates that 2-propanol completely covered the catalysts surface for a concentration equal to 3 mM giving rise to a paramount absorption in the pseudo-liquid phase [5,6], and consequently the reaction rate became of pseudo-zero order [34].

Therefore, the rate of propene formation can be written as:

$$r = k_0 \quad (1)$$

in which "k_0" is the pseudo-zero order rate constant of the reaction.

The apparent activation energies E_a and the pre-exponential factors A were determined from the Arrhenius equation in the form:

$$\ln r = \ln k_0 = \ln A - \frac{E_a}{RT} \quad (2)$$

Eq. (2) has been applied for the runs carried out both in the presence and in the absence of UV-light by using both the bare and the supported HPA materials in the catalytic or the photocatalytic reaction. Figs. 9 and 10 report the Arrhenius plots for all of the runs. The values of E_a and ln A estimated by means of these plots are reported in Table 2.

The values of E_a calculated in the presence of UV light (photocatalytic) were always lower than those estimated under dark conditions (catalytic), justifying the higher reactivity observed in the photocatalytic reactions, as shown in Table 2. It can be observed that the value of E_a for P_2W_{18}/SiO_2 under irradiation decreased more significantly (13.6%) than for P_2W_{18}/TiO_2 (6.5%), although the photoreactivity for the last sample appeared to be always higher. This apparent contradictory result can be explained by taking into account that the percentage decrease under irradiation of the pre-exponential factor A, which is related to physico-chemical factors as adsorption/desorption of reagent and products, was also higher for P_2W_{18}/SiO_2 (9.6%) than for P_2W_{18}/TiO_2 (3.1%). Notably, this factor influences the kinetic constant in the opposite way to E_a as before reported [34].

4. Conclusions

Catalytic and photocatalytic tests for 2-propanol dehydration to propene were successfully carried out by using bare SiO_2 or TiO_2 supported Keggin and Wells-Dawson HPAs. The Wells-Dawson heteropolyacid presented a higher catalytic and photocatalytic activity than the Keggin one particularly when supported. The UV irradiation increased the activity of both HPAs. The heteropolyacid species played a key role both for the catalytic and the photocatalytic reactions, indicating that the acidity of the cluster accounts for the catalytic role (P_2W_{18} showed higher activity with respect to PW_{12} because of the presence of higher amount of acid sites), whereas both the acidity of the cluster and the oxidant ability of excited PW_{12} and P_2W_{18} were responsible for the increase of the reaction rate of the photocatalytic reaction. Moreover, the presence of TiO_2, used as a photoactive semiconductor support, showed a beneficial effect to enhance the reactivity of the binary materials. Finally, the apparent activation energy of 2-propanol catalytic and photocatalytic dehydration, determined in the range 60–120 °C, decreased in the presence of light for all of the (photo)catalysts used.

Acknowledgements

The authors wish to thank Prof. Anna Micek-Ilnicka for fruitful suggestions and MIUR (Rome) and Università degli Studi di Palermo for financial support.

References

[1] M.T. Pope, A. Müller, Angew. Chem. Int. Ed. Engl. 30 (1991) 34–48.
[2] S.S. Wang, G.Y. Yang, Chem. Rev. 115 (2015) 4893–4962.
[3] E. Papaconstantinou, Chem. Soc. Rev. 18 (1989) 1–33.
[4] E.I. García-López, G. Marcì, L. Palmisano, Heterogeneous Photocatalysis: From Fundamentals to Green Applications, in: J.C. Colmenares, Y.J. Xu (Eds.), Springer-Verlag, Berlin Heidelberg, 2016, pp. 63–107.
[5] N. Mizuno, M. Misono, Chem. Rev. 98 (1998) 199–218.
[6] T. Okuhara, N. Mizuno, M. Misono, Adv. Catal. 41 (1996) 113–252.
[7] L.E. Briand, G. Baronetti, H.J. Thomas, Appl. Catal. A 256 (2003) 37–50.
[8] S. Shikata, M. Misono, Chem. Commun. (1998) 1293–1294.
[9] G. Baronetti, L. Briand, U. Sedran, H.J. Thomas, Appl. Catal. A 172 (1998) 265–272.
[10] A. Micek-Ilnicka, J. Mol. Catal. 308 (2009) 1–14.
[11] I.V. Kozhevnikov, Catalysis for Fine Chemical Synthesis. Vol. 2: Catalysis by Polyoxometalates, John Wiley and Sons, Chichester, 2002.
[12] F. Cavani, C. Comuzzi, G. Dolcetti, E. Etienne, R. Finke, G. Selleri, F. Trifirò, A. Trovarelli, J. Catal. 160 (1996) 317–321.
[13] S. Shikata, T. Okuhara, M. Misono, J. Mol. Catal. A 100 (1995) 49–59.
[14] G. Marcì, E.I. García-López, L. Palmisano, Eur. J. Inorg. Chem. (2014) 21–35.
[15] H. Park, W. Choi, J. Phys. Chem. B 107 (2003) 3885–3890.
[16] T. Tachikawa, M. Fujitsuka, T. Majima, J. Phys. Chem. C 111 (2007) 5259–5275.
[17] A. Hiskia, M. Athanasios, E. Papacostantinou, Chem. Soc. Rev. 30 (2001) 62–69.
[18] M. Yoon, J.A. Chang, Y. Kim, J.R. Choi, K. Kim, S.J. Lee, J. Phys. Chem. B 105 (2001) 2539–2545.
[19] D.K. Lyon, W.K. Miller, T. Novet, P.J. Domaille, E. Evitt, D.C. Johnson, R.G. Finke, J. Am. Chem. Soc. 13 (1991) 7209–7221.
[20] C.R. Graham, R.G. Finke, Inorg. Chem. 47 (2008) 3679–3686.
[21] E. Arendt, S. Zehri, P. Eloy, E.M. Gaigneaux, Eur. J. Inorg. Chem. (2012) 2792–2801.
[22] U.B. Mioč, R.Z. Dimitrijević, M. Davidović, Z.P. Nedić, M.M. Mitrović, Ph. Colomban, J. Mater. Sci. 29 (1994) 3705–3718.
[23] G. Marcì, E.I. García-López, M. Bellardita, F. Parisi, C. Colbeau-Justin, S. Sorgues, L.F. Liotta, L. Palmisano, Phys. Chem. Chem. Phys. 15 (2013) 13329–13342.
[24] J.E. Sambeth, G. Romanelli, J.C. Autino, H.J. Thomas, G.T. Baronetti, Appl. Catal. A 378 (2010) 114–118.
[25] G.T. Baronetti, H. Thomas, C.A. Querini, Appl. Catal. A 217 (2001) 131–141.
[26] C. Rocchiccioli-Deltcheff, M. Fournier, R. Franck, R. Thouvenot, Inorg. Chem. 22 (1983) 207–216.
[27] A. Bridgeman, Chem. Phys. 287 (2003) 55–69.
[28] L.M. Martínez-Tejada, A. Muñoz, M.A. Centeno, J. A: Odriozola, J. Raman, Spectroscopy 47 (2016) 189–197.
[29] M.L. Testa, V. La Parola, F.L. Liotta, A.M. Venezia, J. Mol. Catal. A 367 (2013) 69–76.
[30] M.N. Timofeeva, Appl. Catal. A 256 (2003) 19–35.
[31] G. Martra, Appl. Catal. A 200 (2000) 275–285.
[32] A. Bielański, A. Micek-Ilnicka, Inorg. Chem. Acta 363 (2010) 4158–4162.
[33] E.I. García-López, G. Marcì, F.R. Pomilla, A. Micek-Ilnicka, A. Kirpsza, L. Palmisano, Appl. Catal. B 189 (2016) 252–265.
[34] G.C. Bond, S.J. Frodsham, P. Jubb, E.F. Kozhevnikova, I.V. Kozhevnikov, J. Catal. 293 (2012) 158–164.